LASER INTERFEROMETER GRAVITATIONAL WAVE OBSERVATORY

– LIGO –

CALIFORNIA INSTITUTE OF TECHNOLOGY
MASSACHUSETTS INSTITUTE OF TECHNOLOGY

Document Type	**LIGO-T000121-00-R**	**11/7/00**

Determining Lengths and Optical Parameters for Dual Recycling at the 40m LIGO Prototype

Ted Jou, Alan Weinstein

Distribution of this draft:

This is an internal working note
Of the LIGO Project

California Institute of Technology
LIGO Project – MS 51-33
Pasadena, CA 91125
Phone (626)395-2129
Fax (626)304-9834
E-mail: info@ligo.caltech.edu

Massachusetts Institute of Technology
LIGO Project – MS 20B-145
Cambridge, MA 01239
Phone (617)253-4824
Fax (617)253-7014
E-mail: info@ligo.mit.edu

WWW: http://www.ligo.caltech.edu

Determining Lengths and Optical Parameters for Dual Recycling at the 40m LIGO Prototype

Ted Jou
Dr. Alan Weinstein, mentor

Abstract

The next phase of the LIGO project will allow tuning of a specific frequency to amplify the gravitational wave signal. The LIGO II design accomplishes this by using an extra mirror to implement a dual recycling configuration. Appropriate parameters (mirror reflectivities, cavity lengths, RF modulation frequencies) need to be determined to implement and test this setup at the 40m LIGO Prototype. Twiddle, a Mathematica program for modeling LIGO-like interferometers, was used to find lengths and optical parameters that optimize the frequency response of the interferometer and provide a functional length-sensing scheme.

Introduction

The Laser Interferometer Gravitational-wave Observatory (LIGO) is a facility dedicated to the detection of cosmic gravitational waves. The construction and operation of LIGO is a collaborative effort between Caltech and MIT with funding from the National Science Foundation (NSF). The two detectors that make up LIGO are located in Hanford, WA and Livingston, LA. The primary prototype for these detectors is the 40m LIGO Prototype, which is located at Caltech.

Gravitational waves are ripples in space-time predicted by Einstein's 1916 general theory of relativity. However, these waves have never been detected and their direct measurement is the main purpose of LIGO. A gravitational wave is emitted by accelerating masses, and a large gravity wave with a detectable signal could be emitted by interacting black holes or neutron stars. A gravitational wave interacts with LIGO by distorting space-time in a very specific way. The LIGO detectors are designed to measure this distortion as accurately as possible.

At the current stage of the LIGO project, known as LIGO I, the detectors are power-recycled Michelson interferometers with 4km long Fabry-Perot arms. This optical configuration, shown in Figure 1, measures a gravitational wave's distortion of space-time as a difference in the lengths of its two arms. The Michelson interferometer configuration allows this measurement to be made. The main component of a Michelson interferometer is a beam splitter, which takes the input light and sends half of it into each of two perpendicular arms. If the two arms of a Michelson interferometer are the exact same length, light coming back from the arms will interfere constructively in one direction and destructively in the other direction, creating a bright port and a dark port. If the arms differ in length by even a small amount, as in the case of a space-time distortion by a gravitational wave, this phenomenon ceases to occur and a signal can be detected at the dark port.

The magnitude of this signal is greatly dependent upon two factors, the input light power and the magnitude of the length change in the arms. Placing a mirror at the bright

port can increase the light power by recycling light back into the interferometer and is called power-recycling. Simply making an interferometer with longer arms can amplify a small length change. For this reason, the LIGO detectors have 4km long arms. In addition to making the arms physically longer, the optical path can be folded on top of itself to effectively multiply the length of the arm several times. This is accomplished by creating Fabry-Perot arm cavities in the arms, letting light resonate between an input and end mirror. The two mirrors that make up the Fabry-Perot arms are the test masses – they move in response to changes in the gravitational field and it is this movement that provides the length change related to a gravitational wave signal.

Since very small changes in the lengths of the arms cause a signal to appear in the dark port, the interferometer is very sensitive to spurious mirror movements. Thus, there must be some scheme that can control this noise and isolate the gravitational wave signal. The entire optical setup sits inside a vacuum on a seismic isolation stack, so using any external components to monitor this noise would disturb this noise-free environment. Thus, the sensing system must utilize only the optics already in the interferometer. In 1991, S. Whitcomb proposed a scheme that could accomplish this task (ISC, 1998). By phase modulating the laser light at a radio frequency, two sidebands are put on the light, one above the carrier frequency and one below it. The lengths of various parts of the interferometer are then adjusted to set the resonance characteristics of the sidebands and the carrier. Then, by monitoring the carrier and sideband signals at different parts of the interferometer, the distances between all the mirrors can be monitored.

To understand how this works, the interferometer needs to be broken down into three cavities, shown in Figure 2. Between the power-recycling mirror and the input test masses is the power-recycling cavity. The two Fabry-Perot arms are the other two cavities. Depending on the length of a cavity, a certain frequency light will have a specific tune, corresponding to the number of wavelengths of light in the length of the cavity. When the tune is an integer, the light is resonant: it interferes constructively with itself and causes a power gain; when the tune is a half-integer, the light is anti-resonant: it interferes destructively and causes a power loss. Consequently, a small length change near resonance will cause a large change in the power and phase of the light while length changes near anti-resonance will cause very little change in power. These facts allow the sidebands to provide information about the distances between mirrors in the interferometer.

Since there is no way to tell whether the lengthening or shortening of a single arm is due to a gravitational wave or some noise source, the distances between the mirrors needs to be broken down into degrees of freedom that separate out the gravitational wave signal. The effect that a gravitational wave will have on the LIGO interferometer is a lengthening of one arm coinciding with a shortening of the other arm. This degree of freedom is designated L-, the differential length of the arms. To define the lengths of the arms, another degree of freedom, L+, the common length of the arms, must be defined. Any change in L+ must be due to noise since a gravitational wave cannot cause this sort of motion. Within the power-recycling cavity, there are corresponding l+ and l-, common and differential Michelson degrees of freedom. These four degrees of freedom define the lengths of the three cavities.

Differentiating between these signals using only the carrier and the sidebands is rather complicated, but relies on fixing the resonance conditions of the sidebands in the

cavities. The carrier is resonant in both the power-recycling and arm cavities. The sidebands on the other hand, are resonant in the power-recycling cavity but anti-resonant in the arms. Also, some asymmetry is put into the interferometer so that the sidebands leak out the dark part. With these characteristics, the values of the electric field at a few points in the interferometer can reveal the values of each of the degrees of freedom.

In the LIGO I length sensing scheme, summarized in Figure 2, photodiodes are placed before the recycling mirror, inside the power-recycling cavity, and at the dark port – the symmetric, pickoff, and asymmetric ports, respectively. At each port, the signals from the sidebands and carrier can be demodulated at two phases, inphase and quadphase. The L+ and l+ signals come from the inphase symmetric and pickoff signals. The L- signal comes from the quadphase asymmetric, and the l- from the quadphase symmetric and pickoff signals.

In the next stage of the LIGO project, LIGO II, the detectors will have a different optical layout. The LIGO II detectors will be *dual*-recycled Michelson interferometers with Fabry-Perot arms. The only change in the optics from the LIGO I configuration is the addition of a signal-recycling mirror at the dark port. This mirror will increase the power of the gravitational wave signal at the dark port, making smaller L- signals detectable. This additional mirror adds another cavity, the signal-recycling cavity, and its length must be monitored along with the arms and the power-recycling cavity. This new degree of freedom is designated s+. A scheme for monitoring this degree of freedom in addition to the previous four requires additional sidebands, which makes the control scheme much more complicated.

The main benefit of the dual-recycling scheme is the ability to recycle a gravitational wave signal. However, it can only recycle one frequency of signal at a time, so it is most useful for events with known frequencies, such as pulsars. As with all cavities, the resonant frequency is dependent upon the length of the cavity. Thus, by adjusting the length of the signal-recycling cavity, the interferometer can be detuned to look at a gravitational wave event of a particular frequency.

This LIGO II configuration must be implemented at the 40m prototype with a working length sensing and control system. This will verify the feasibility of this system for use at the LIGO 4km detectors. One length-sensing scheme, developed by Jim Mason, uses a set of RF sidebands and a frequency-shifted subcarrier. The sidebands are resonant in the power-recycling cavity and the subcarrier is resonant in both the power-recycling cavity and the signal. Using the same photodiodes, all the relevant degrees of freedom can be monitored.

Materials and Methods

Before any optical configuration can be implemented at the 40m or at LIGO II, a mathematical model must be created to predict the length sensing signals that will be expected. A Mathematica package called Twiddle, written by James Regehr, James Mason, and Hiro Yamamoto for modeling LIGO-like interferometers, can be used to simulate the response of a particular interferometer configuration to different mirror motions. Within the model, various optical parameters and lengths can be varied to optimize the response of the interferometer to the degrees of freedom which are important. Only after these signals are optimized is the optical configuration implemented in a real interferometer.

The parameters inputted into a Twiddle model are the modulation frequencies of the sidebands, the tune of the carrier light in each cavity, the layout, optical parameters, and distances between each mirror. These parameters define the static interferometer and Twiddle can calculate the electric fields at every position in the interferometer. Then, mirrors in the interferometer can be shaken at specific frequencies and electric fields can be monitored to find transfer functions. Cavities can also be swept to find the DC error signals for the different degrees of freedom.

For the model of Jim Mason's length sensing scheme, the parameters in Appendix A were used. The modulation frequencies in the source characteristics were chosen to be resonant in the mode cleaner. The length of the PRC, SRC, and arms were based upon these modulation frequencies, keeping the sidebands and subcarrier resonant or anti-resonant in the right cavities. The mirror reflectivities were based on existing optics and were did not deviate far from the LIGO I values. Free parameters, such as the Schnupp asymmetry, δ, were adjusted to optimize the pertinent length sensing signals, which can be seen in Appendix B and are discussed below in the Results section. The ν symbol represents the detuning of the interferometer, which ranges from 0 to 1. The length of the SRC is shown as a formula because it is completely dependent upon the detuning value and the modulation frequency of the subcarrier; the subcarrier must be kept resonant in the SRC while the tune of the carrier changes.

Results

The interferometer lengths and optical parameters correctly modeled the resonance characteristics of the carrier, sideband, and subcarrier in each cavity, which can be seen in the fields at various ports in the Twiddle model at the end of Appendix A. The arm cavity, being a simple Fabry-Perot cavity, should have an amplitude gain equal to t1/(1-r1r2) for a resonant frequency, where t's represent transissivities, r's reflectivities, and 1 and 2 the two ends of the cavity. Using the given reflectivity and transmissivity values in Appendix A(which are in terms of power, thus their square roots give the amplitude values), this expression evaluates to 11.426. The power gain that Twiddle finds is 909.038/6.94712 = 130.851. $\sqrt{130.851} = 11.426$, so Twiddle agrees with the theoretical model exactly. The reflectivity of a Fabry-Perot cavity is given by (r1-r2)/(1-r1r2) for a resonant frequency. This gives an amplitude reflectivity of –0.9977. Using this value, a Fabry-Perot cavity can be defined with the compound mirror of the arms at one end and the power-recycling mirror at the other. This predicts a power gain of 4.155. The power gain that Twiddle calculates is 13.9047/0.833383 = 4.085. These are also very close, but there is a discrepancy due to losses in the beam splitter that prevent the power-recycling cavity from being a perfect Fabry-Perot . A power gain can also be seen for the sidebands and subcarrier in the power-recycling cavity, and at the dark port for the subcarrier. Also, there is a power drop in the arms, illustrating the resonance characteristics of these frequencies throughout the interferometer. These values can be predicted in the same way as the carrier, and also verify the validity of the Twiddle model.

Using the features of Twiddle, any longitudinal motion of a mirror can be simulated while the output at any position in the interferometer is monitored. This provides the signals that are associated with each degree of freedom. Two graphs can be

generated, a DC error signal, resulting from a sweep of the cavity length; and a Bode plot, showing the slope of that error signal at different frequencies of mirror motion. All units of cavity length are in wavelengths of the carrier light (λ, which will be 1.064 μm at the 40m) and the powers are in $W/(\lambda/2\pi)$, where the laser input is normalized to 1 W. The error signals and Bode plots for each degree of freedom are found in Appendix B.

The slopes of the DC plots give the magnitude of the error signals that can be expected for each degree of freedom. If these values can be put into a diagonal matrix, the signals will be easily coordinated with their respective degree of freedom. The matrix for this configuration is nearly diagonal and can be found at the end of Appendix B.

The signal-recycling properties of this optical configuration can also be investigated with the Twiddle model. By varying the length of the signal-recycling cavity, the interferometer can be detuned to different gravitational wave frequencies. By looking at the Bode plot for the L- signal, this detuning can be seen as a resonance peak in the graph. A chart and graph of these detunings can be found in Appendix C. The SRC length values are derived from the formula found in Appendix A. The resonance peaks are determined simply by inspection of the Bode plots. The two extreme detunings are signal recycling, $\nu=1$, at the extreme left of the graph, where the power gain is the highest, and resonant sideband extraction, $\nu=0$, at the extreme right, where signals are visible across the widest range of frequencies.

Discussion

Parameters were found for the Twiddle model that provided workable length sensing signals and exhibited signal-recycling behavior across a wide range of frequencies. This shows that Jim Mason's scheme is good enough to implement at the 40m interferometer.

The error signals all show an approximately linear behavior around perfect alignment, which makes it easier to design feedback systems to stabilize the lengths of the cavities when they fall away from their desired value. In most of the error signals, there is a minimum of other zero crossings, so that it will be apparent to the control plant that it is centering the length of the cavity on the correct value.

In the DC Matrix, the numbers in bold are the signals that appear most useful for each degree of freedom. There are 0's and small numbers for many signals that share rows and columns with the chosen signals, which is good because it reduces the amount of noise that enters into each error signal. In most cases, they are the largest values in their row, so that if a signal appears at a particular frequency and phase, it can be identified with the appropriate degree of freedom. In cases where two signals share a row, a gain hierarchy can be set up to filter out the smaller signal (Regehr, 1994).

The signal-recycling characteristics show a well-defined peak for a very wide range of frequencies. At the 40m however, only the frequencies below ~1000 Hz will have visible peaks because other noise sources obscure the higher frequencies. Thus, the 40m dual-recycling configuration will have to operate very near the signal recycling limit, where $\nu=1$.

With a working Twiddle model, parameters can be varied to reflect changes in components or configurations without much effort. The model is very flexible and will be useful even if dramatic changes occur to the interferometer plan.

Conclusion

A model of the 40m LIGO prototype in a dual-recycling configuration was successfully created using Twiddle. A length sensing scheme, developed by Jim Mason, was implemented in this model and the resulting values from this scheme were simulated and recorded. The signal-recycling capability of the configuration was verified. The lengths and optical parameters of the interferometer were varied to optimize the length sensing signals and the signal-recycling properties of the system. These parameters can now be implemented at the 40m LIGO prototype and eventually at the 4km LIGO detectors.

Since the completion of this project, the most likely length sensing scheme for LIGO II has been changed. There will no longer be a subcarrier, but rather, a second set of sidebands with modulation frequency many times that of the first sidebands. The first set of sidebands have the same resonance characteristics as the original sidebands and the second set of sidebands arm the same as the subcarrier. There will also be a DC offset put into the arms to allow some carrier to leak out the dark port. The other characteristics of the system are very similar, but the optimal parameters will be different, so this scheme needs to be modeled with Twiddle before implementation at the 40m.

Acknowledgements

I would like to thank the National Science Foundation and Mr. Jeffrey Jacob at Meta Probe for providing the funds for my SURF this summer. I would also like to thank Steve Vass and Dennis Ugolini at the 40m for working with me this summer; also, my fellow SURF students in the 40m, Lisa, Ivica, Jitesh, and Brian for making the summer more fun. Many thanks go to my mentor, Alan Weinstein, for getting me into this project and for providing me guidance and motivation throughout the project. Finally, I'd like to thank Jim Mason for his expert knowledge in this area and for the time he spent sharing it with me.

Bibliography

DeSalvo, Riccardo. "The Quest for Gravitational Waves". CERN Courier: March 1999.

ISC Team, "Length Sensing & Control Subsystem Final Design". LIGO Design Document. LIGO-T980068-00. 1998.

Regehr, Martin W. "Signal Extraction and Control for an Interferometric Gravitational Wave Detector". Ph.D Thesis, California Institute of Technology. LIGO-P940002-00-I. August, 1994.

Regehr, Martin; Mason, James; and Yamamoto, Hiro. "Twiddle - A Program for Analyzing Interferometer Frequency Response". LIGO Project. LIGO-T990022-00-R. 1999.

Weinstein, Alan. "Calculation of Cavity Lengths and RF Frequencies for RSE at the 40m". LIGO Working Document. January 17, 2000.

Figures

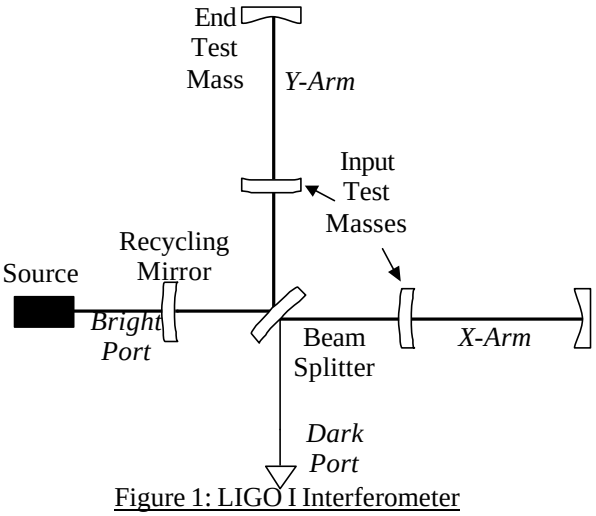

Figure 1: LIGO I Interferometer

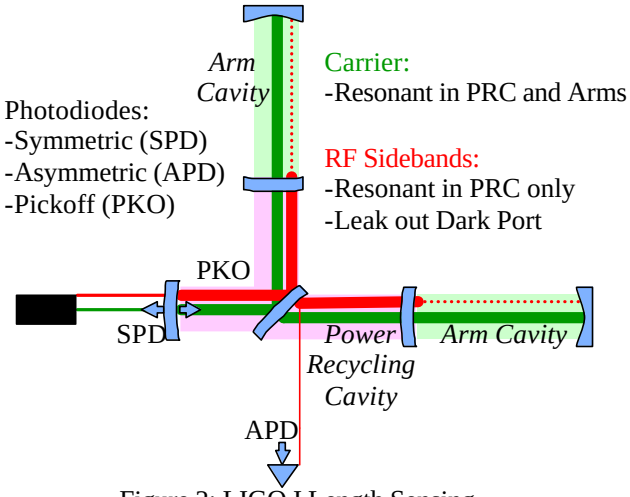

Figure 2: LIGO I Length Sensing

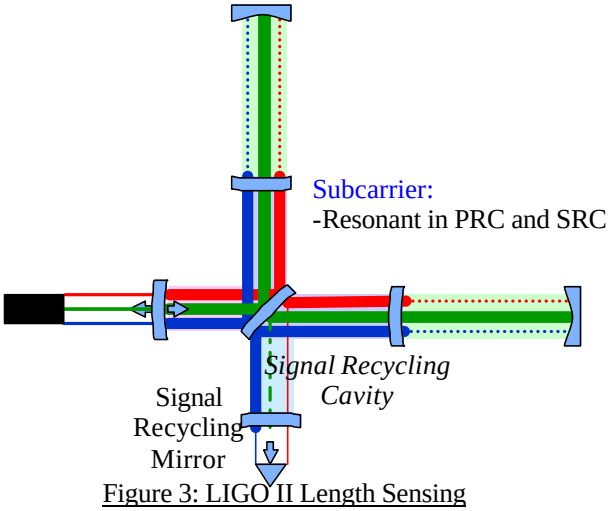

Figure 3: LIGO II Length Sensing

Appendix A

Source	Freq (MHz)	Amplitude
SB-	-36.6868	0.235667i
Carrier	0	0.912898
SB+	36.6868	0.235667i
SubCarr	110.06	0.235667i

Mirror	Reflect	Trans	Loss
Recycl	0.79998	0.2	2E-5
BmSpl	0.499625	0.5	7.5E-4
ITM	0.96998	0.03	2E-5
ETM	0.999965	1.5E-5	2E-5
Signal	0.79998	0.2	2E-5

Lengths	
lprc	2.04292m
d	0.337081m
larm	38.8154m
lsrc	$c/4\times(110.06)\times(5-\nu)$

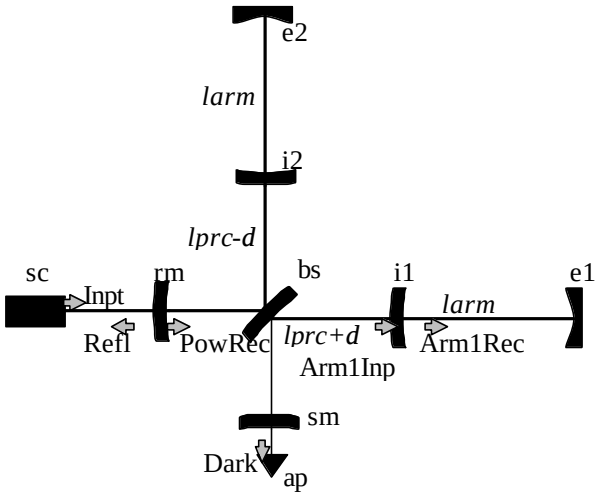

Figure A: Twiddle Model Components

Tune (´ p/2)	PRC	Arms	SRC
Carrier	2n	2n+1	ν
SB – Carr	3	19	(5–ν)/3
Sub – Carr	9	57	5–ν

Ports		Power (W)	Phase				
Inpt	Carrier	0.833383	0	Arm1Inp	Carrier	6.94712	0
	SB's	0.055539	π/2		SB's	~0.1	-
	SubCarr	0.055539	π/2		SubCarr	~0.25	-
Refl	Carrier	0.712046	0				
	SB's	~0.04	-				
	SubCarr	0.0000043	π/2				
PowRec	Carrier	13.9047	0	Arm1Rec	Carrier	909.038	0
	SB's	~0.2	-		SB's	~0.001	-
	SubCarr	0.282050	π/2		SubCarr	~0.002	-
Dark	Carrier	0	νπ/2				
	SB's	~0.01	-				
	SubCarr	0.054762	π				

Appendix B

Figure B1: Common Arm (L+):

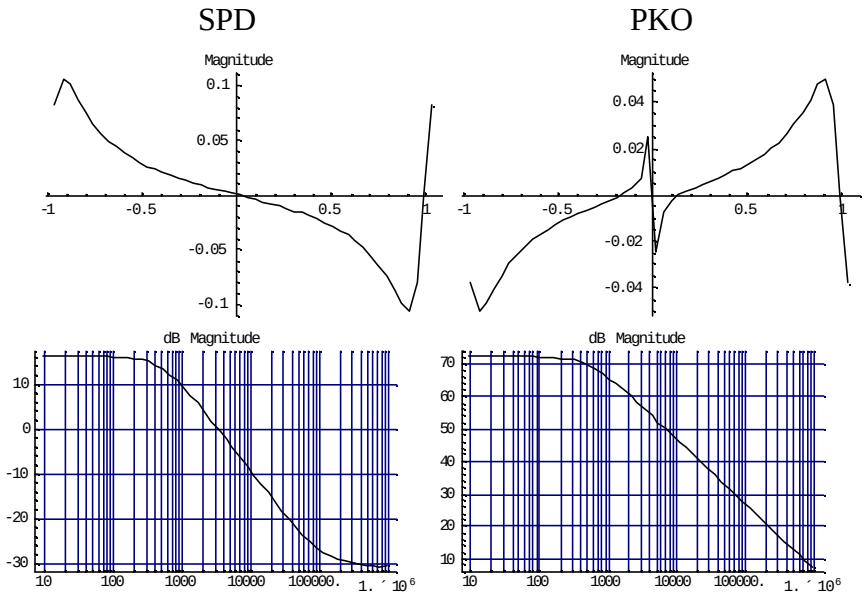

Figure B2: Differential Arm (L-):

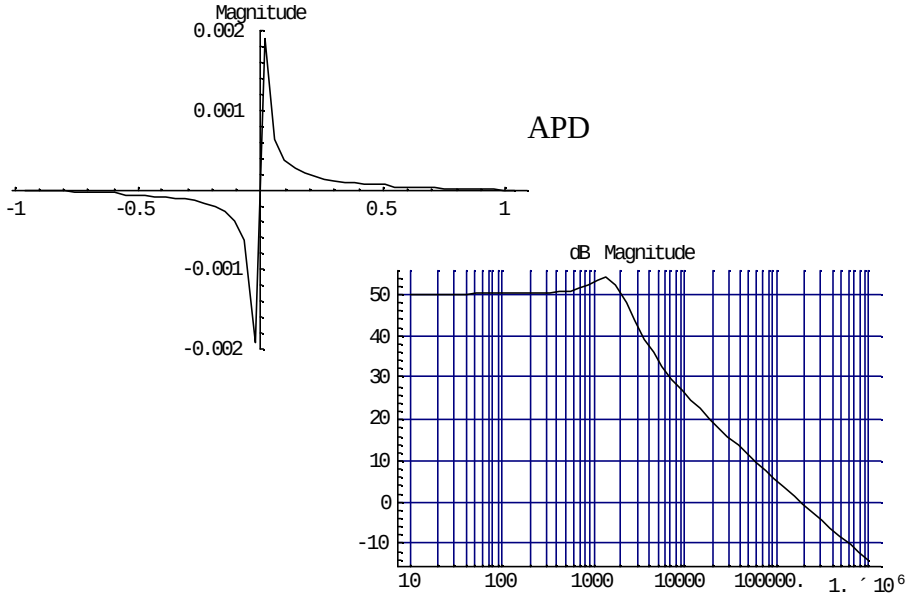

Figure B3: Common Michelson (l+):

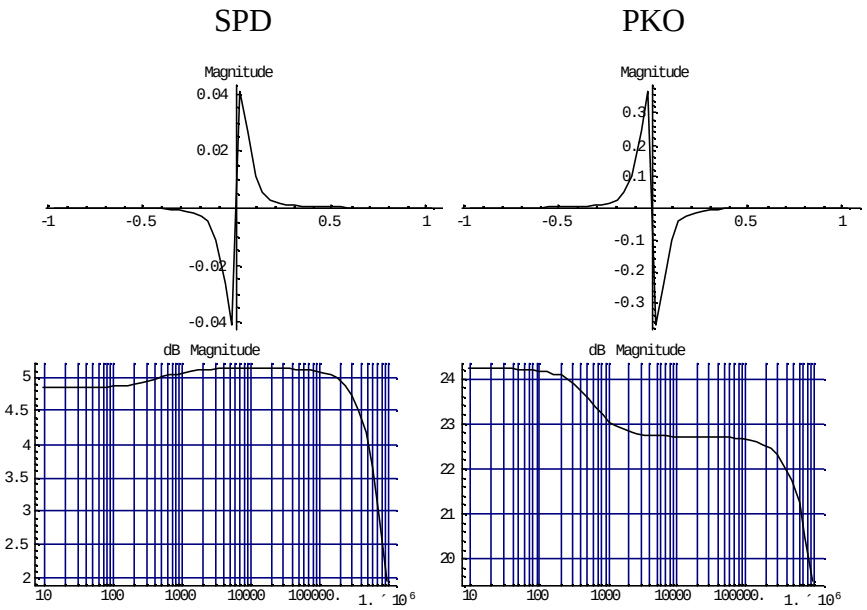

Figure B4: Differential Michelson (l-):

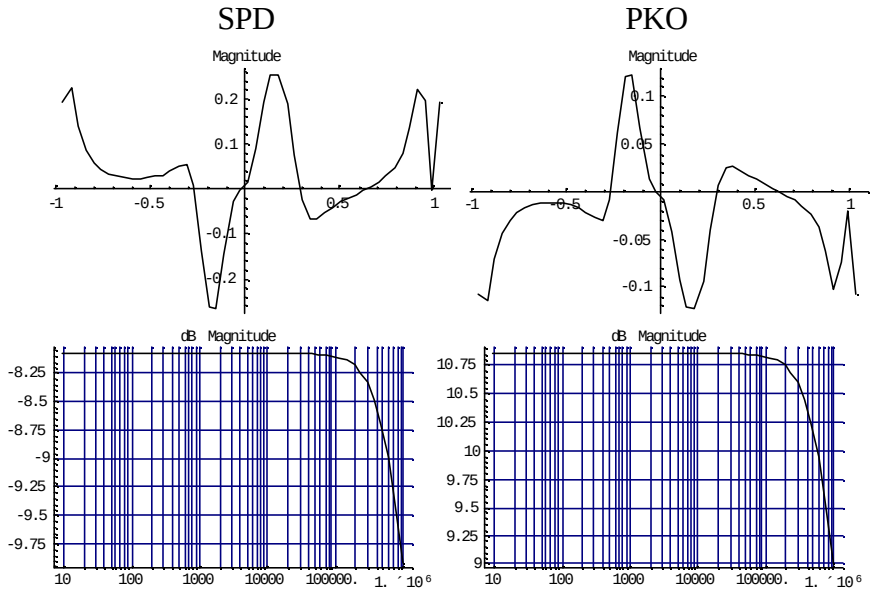

Figure B5: Common Signal Recycling (s+)

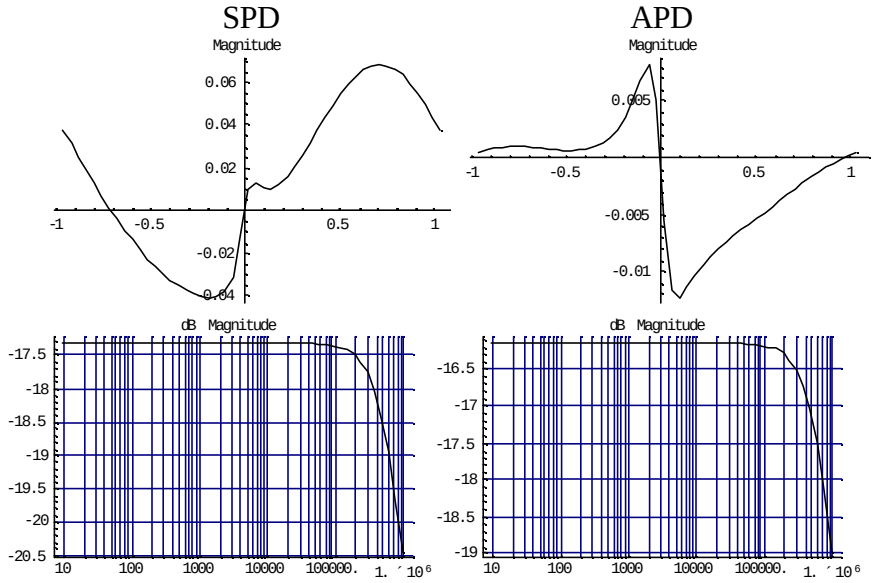

Table B: DC Matrix:

Freq	Phase	PD	L+	L-	l+	l-	s+
36.6868 MHz	0.19π	SPD	1516.95	0.014876	-9.33915	**1.95352**	-0.565124
		PKO	-922.376	0.13147	26.5742	**17.2651**	-4.99453
	0	APD	0	56.4169	0	0.429603	0
110.06 MHz		SPD	**-8.19106**	0	**-1.74752**	0	1.75378
		PKO	**-4230.34**	0	**16.2174**	0	15.4998
	0.39π	APD	0	**324.076**	0	2.46777	0
73.3736 MHz	1.78π	SPD	0.000189	0.000033	0.111518	0.004317	**0.136336**
	1.32π	PKO	0.026592	-0.00327	-2.18296	-0.429417	1.3092
	0.11π	APD	-0.00179	-0.00044	0.079241	-0.057963	**-0.155943**

Appendix C

Table C: Detunings, SRC Lengths, and Pole Frequencies:

ν	1	0.98	0.97	0.96	0.95	0.93	0.9
SRC (m)	2.7239	2.7375	2.7443	2.7511	2.7579	2.7716	2.7920
Pole (kHz)	0	0.28	0.43	0.53	0.67	1.1	1.4

ν	0.8	0.7	0.5	0.3	0.2	0.1	0
SRC (m)	2.8601	2.9282	3.0644	3.2006	3.2687	3.3368	3.4049
Pole (kHz)	2.8	3.4	9.5	18	30	60	300

Figure C: L- Bode Plots: